

Chapter 5

Data Format and Pulse Shape Classification

Marvin K. Simon and Dariush Divsalar

In autonomous radio operation, aside from classifying the modulation type, e.g., deciding between binary phase-shift keying (BPSK) and quadrature phase-shift keying (QPSK), it is also desirable to have an algorithm for choosing the data format, e.g., non-return to zero (NRZ) versus Manchester encoding. We will see in our discussions of carrier synchronization in Chapter 8 that, in the absence of subcarriers, when NRZ is employed along with a residual carrier, the carrier-tracking loop takes a loss due to overlapping carrier and modulation spectra, whereas Manchester coding may use either suppressed or residual carrier without such a loss. With this consideration in mind, we shall consider two different scenarios. In one case, independent of the data format, the modulations are assumed to be fully suppressed carrier. In the other case, which is typical of the current Electra radio design, an NRZ data format is always used on a fully suppressed carrier modulation whereas a residual carrier modulation always employs Manchester-coded data. In the latter case, the data format classification algorithm and its performance clearly will be a function of the modulation index, i.e., the allocation of the power to the discrete and data-modulated signal components. Estimation of the modulation index was discussed in Chapter 3.

In this chapter, we derive the maximum-likelihood (ML)-based data format classification algorithms as well as reduced-complexity versions of them obtained by applying suitable approximations of the nonlinearities resulting from the ML formulation. As in previous classification problems of this type, we shall first assume that all other system parameters are known. Following this, we relax the assumption of known carrier phase and, as was done for the modulation classification discussion, we shall consider the noncoherent version of the ML

classifiers. Numerical performance evaluation will be obtained by computer simulations and, wherever possible, by theoretical analyses to verify the simulation results.

5.1 Coherent Classifiers of Data Format for BPSK

5.1.1 Maximum-Likelihood Coherent Classifier of Data Format for BPSK

We begin by considering suppressed-carrier BPSK modulation and a choice between NRZ and Manchester encoding. Thus, the received signal is given by Eqs. (1-3) and (1-6), or in passband by

$$r(t) = \sqrt{2P} \left(\sum_{n=-\infty}^{\infty} c_n p(t - nT) \right) \cos \omega_c t + n(t) \quad (5-1)$$

where P is the signal power,¹ $\{c_n\}$ is the sequence of binary independent, identically distributed (iid) data taking on values ± 1 with equal probability, $p(t)$ is the pulse shape (the item to be classified), ω_c is the radian carrier frequency, $1/T$ is the data (symbol) rate, and $n(t)$ is a bandpass additive white Gaussian noise (AWGN) source with single-sided power spectral density N_0 W/Hz. Based on the above AWGN model, then for an observation of K data intervals, the conditional-likelihood function (CLF) is given by

$$\begin{aligned} p(r(t)|\{c_n\}, p(t)) &= \frac{1}{\sqrt{\pi N_0}} \exp \left(-\frac{1}{N_0} \int_0^{KT} \left[r(t) - \sqrt{2P} \left(\sum_{n=-\infty}^{\infty} c_n p(t - nT) \right) \cos \omega_c t \right]^2 dt \right) \\ &= C \exp \left(\frac{2\sqrt{2P}}{N_0} \sum_{k=0}^{K-1} c_k \int_{kT}^{(k+1)T} r(t) p(t - kT) \cos \omega_c t dt \right) \\ &= C \prod_{k=0}^{K-1} \exp \left(\frac{2\sqrt{2P}}{N_0} c_k \int_{kT}^{(k+1)T} r(t) p(t - kT) \cos \omega_c t dt \right) \end{aligned} \quad (5-2)$$

¹ There is no need to distinguish between total and data power here since in the suppressed-carrier case all of the signal power is allocated to the data modulation. Thus, for simplicity of notation, we shall simply use P without a subscript to denote signal power.

where C is a constant that has no bearing on the classification. Averaging over the iid data sequence gives

$$p(r(t)|p(t)) = C \prod_{k=0}^{K-1} \cosh \left(\frac{2\sqrt{2P}}{N_0} \int_{kT}^{(k+1)T} r(t)p(t-kT) \cos \omega_c t dt \right) \quad (5-3)$$

Finally, taking the logarithm of Eq. (5-3), we obtain the log-likelihood function (LLF)

$$\Lambda \triangleq \ln p(r(t)|p(t)) = \sum_{k=0}^{K-1} \ln \cosh \left(\frac{2\sqrt{2P}}{N_0} \int_{kT}^{(k+1)T} r(t)p(t-kT) \cos \omega_c t dt \right) \quad (5-4)$$

where we have ignored the additive constant $\ln C$.

For NRZ data, $p(t)$ is a unit rectangular pulse of duration T , i.e.,

$$p_1(t) = \begin{cases} 1, & 0 \leq t \leq T \\ 0, & \text{otherwise} \end{cases} \quad (5-5)$$

For Manchester-encoded data, $p(t)$ is a unit square-wave pulse of duration T , i.e.,

$$p_2(t) = \begin{cases} 1, & 0 \leq t \leq T/2 \\ -1, & T/2 \leq t \leq T \end{cases} \quad (5-6)$$

Thus, defining the received observable

$$\begin{aligned} r_k(l) &\triangleq \int_{kT}^{(k+1)T} r(t)p_l(t-kT) \cos \omega_c t dt \\ &= \begin{cases} \int_{kT}^{(k+1)T} r(t) \cos \omega_c t dt; & l = 1 \\ \int_{kT}^{(k+1/2)T} r(t) \cos \omega_c t dt - \int_{(k+1/2)T}^{(k+1)T} r(t) \cos \omega_c t dt; & l = 2 \end{cases} \end{aligned} \quad (5-7)$$

then a classification choice between the two pulse shapes based on the LLF would be to choose Manchester if

$$\sum_{k=0}^{K-1} \ln \cosh \left(\frac{2\sqrt{2P}}{N_0} r_k(1) \right) < \sum_{k=0}^{K-1} \ln \cosh \left(\frac{2\sqrt{2P}}{N_0} r_k(2) \right) \quad (5-8)$$

Otherwise, choose NRZ.

5.1.2 Reduced-Complexity Data Format BPSK Classifiers

To simplify the form of the classification rule in Eq. (5-8), we replace the $\ln \cosh(\cdot)$ function by its small and large argument approximations. In particular,

$$\ln \cosh x \cong \begin{cases} x^2/2; & x \text{ small} \\ |x| - \ln 2; & x \text{ large} \end{cases} \quad (5-9)$$

Thus, for low signal-to-noise ratio (SNR), Eq. (5-8) simplifies to

$$\begin{aligned} & \sum_{k=0}^{K-1} \left(\int_{kT}^{(k+1)T} r(t) \cos \omega_c t dt \right)^2 \\ & < \sum_{k=0}^{K-1} \left(\int_{kT}^{(k+1/2)T} r(t) \cos \omega_c t dt - \int_{(k+1/2)T}^{(k+1)T} r(t) \cos \omega_c t dt \right)^2 \end{aligned} \quad (5-10)$$

or

$$\sum_{k=0}^{K-1} \int_{kT}^{(k+1/2)T} r(t) \cos \omega_c t dt \int_{(k+1/2)T}^{(k+1)T} r(\tau) \cos \omega_c \tau d\tau < 0 \quad (5-11)$$

For high SNR, Eq. (5-8) reduces to

$$\begin{aligned} & \sum_{k=0}^{K-1} \left| \int_{kT}^{(k+1/2)T} r(t) \cos \omega_c t dt + \int_{(k+1/2)T}^{(k+1)T} r(t) \cos \omega_c t dt \right| \\ & < \sum_{k=0}^{K-1} \left| \int_{kT}^{(k+1/2)T} r(t) \cos \omega_c t dt - \int_{(k+1/2)T}^{(k+1)T} r(t) \cos \omega_c t dt \right| \end{aligned} \quad (5-12)$$

Note that while the optimum classifier of Eq. (5-8) requires knowledge of SNR, the reduced-complexity classifiers of Eqs. (5-10) and (5-12) do not. Figure 5-1 is a block diagram of the implementation of the low and high SNR classifiers defined by Eqs. (5-11) and (5-12).

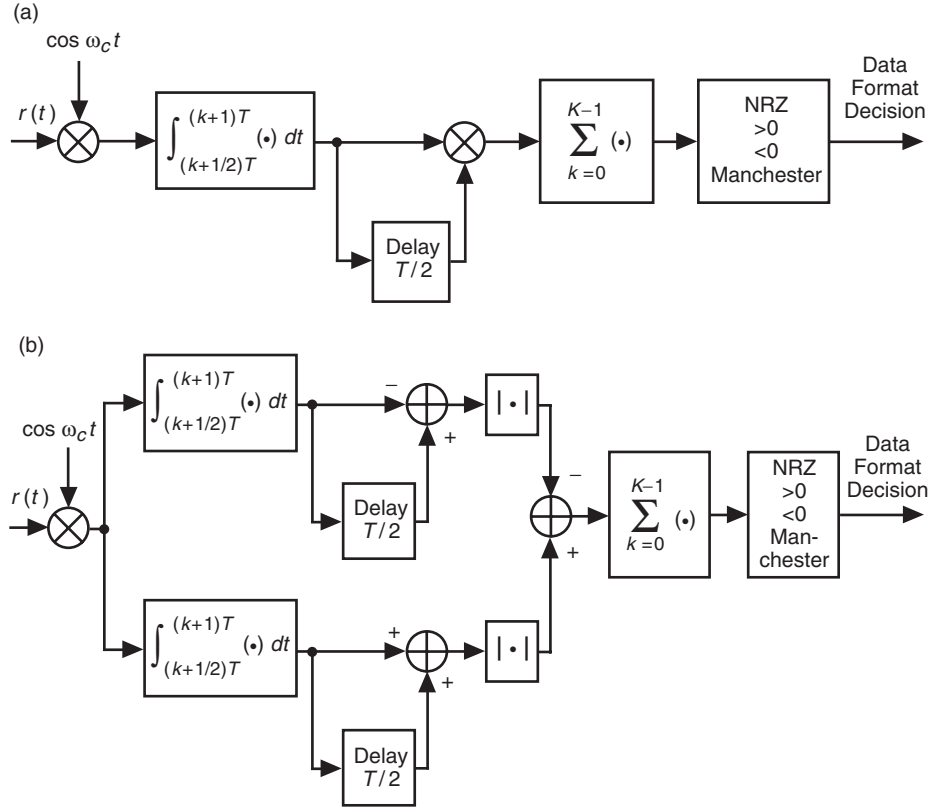


Fig. 5-1. Reduced-complexity coherent data format classifiers for BPSK modulation: (a) low SNR and (b) high SNR.

5.1.3 Probability of Misclassification for Coherent BPSK

5.1.3.1. Exact Evaluation. To illustrate the behavior of the misclassification probability, P_M , with SNR, we consider the low SNR case and evaluate first the probability of the event in Eq. (5-11) given that the transmitted data sequence was in fact NRZ encoded. In particular, we recognize that, given a particular data sequence of K bits,

$$X_{ck} = \int_{kT}^{(k+1/2)T} r(t) \cos \omega_c t dt$$

$$Y_{ck} = \int_{(k+1/2)T}^{(k+1)T} r(\tau) \cos \omega_c t d\tau$$

$k = 0, 1, \dots, K-1$, are mutually independent and identically distributed (iid) Gaussian random variables (RVs). Thus, the LLF

$$D = \sum_{k=0}^{K-1} \int_{kT}^{(k+1/2)T} r(t) \cos \omega_c t dt \int_{(k+1/2)T}^{(k+1)T} r(\tau) \cos \omega_c \tau d\tau = \sum_{k=0}^{K-1} X_{ck} Y_{ck} \quad (5-13)$$

is a special case of a quadratic form of *real* Gaussian RVs and the probability of the event in Eq. (5-11), namely, $\Pr\{D < 0\}$ can be evaluated in closed form by applying the results in [1, Appendix B] and the additional simplification of these in [2, Appendix 9A]. To see this connection, we define the complex Gaussian RVs $X_k = X_{ck} + jX_{c,k+1}$, $Y_k = Y_{ck} + jY_{c,k+1}$. Then, $X_k Y_k^* + X_k^* Y_k = 2(X_{ck} Y_{ck} + X_{c,k+1} Y_{c,k+1})$. Assuming arbitrarily that K is even, then we can rewrite D of Eq. (5-13) as

$$D = \frac{1}{2} \sum_{k=0}^{K/2-1} (X_k Y_k^* + X_k^* Y_k) \quad (5-14)$$

Comparing Eq. (5-14) with [2, Eq. (B.1)], we see that the former is a special case of the latter, corresponding to $A = B = 0, C = 1/2$. Specifically, making use of the first and second moments of X_k and Y_k given by

$$\begin{aligned} \bar{X}_k &= \bar{Y}_k = (c_k + jc_{k+1}) \sqrt{P/8T} \\ \mu_{xx} &= \frac{1}{2} E \left\{ |X_k - \bar{X}_k|^2 \right\} = N_0 T / 8 \\ \mu_{yy} &= \frac{1}{2} E \left\{ |Y_{ck} - \bar{Y}_{ck}|^2 \right\} = N_0 T / 8 \\ \mu_{xy} &= \frac{1}{2} E \left\{ (X_{ck} - \bar{X}_{ck}) (Y_{ck} - \bar{Y}_{ck})^* \right\} = 0 \end{aligned} \quad (5-15)$$

then from [2, Eq. (9A.15)],

$$P_M(1) = \frac{1}{2} + \frac{1}{2^{K-1}} \sum_{k=1}^{K/2} \binom{K-1}{K/2-k} [Q_k(a, b) - Q_k(b, a)] \quad (5-16)$$

where $Q_k(a, b)$ is the k th-order Marcum Q -function and

$$\begin{aligned} a &= \sqrt{\frac{v(\xi_1 v - \xi_2)}{2}} \\ b &= \sqrt{\frac{v(\xi_1 v + \xi_2)}{2}} \end{aligned} \quad (5-17)$$

with

$$\begin{aligned} v &= \sqrt{\frac{1}{\mu_{xx}\mu_{yy}}} = \frac{8}{N_0 T} \\ \xi_1 &= \frac{1}{2} \sum_{k=0}^{K/2-1} \left(|\bar{X}_{ck}|^2 \mu_{yy} + |\bar{Y}_{ck}|^2 \mu_{xx} \right) = \frac{KPT^3 N_0}{64} \\ \xi_2 &= \sum_{k=0}^{K/2-1} |\bar{X}_{ck}| |\bar{Y}_{ck}| = \frac{KPT^2}{8} \end{aligned} \quad (5-18)$$

Substituting Eq. (5-18) into Eq. (5-17) gives

$$\begin{aligned} a &= 0 \\ b &= \sqrt{K(E_s/N_0)} \end{aligned} \quad (5-19)$$

where $E_s = PT$ denotes the signal energy. However,

$$\begin{aligned} Q_k(0, b) &= \sum_{n=0}^{k-1} \exp\left(-\frac{b^2}{2}\right) \frac{(b^2/2)^n}{n!} \\ Q_k(b, 0) &= 1 \end{aligned} \quad (5-20)$$

Thus, using Eqs. (5-19) and (5-20) in Eq. (5-16) gives the desired result:

$$P_M(1) = \frac{1}{2} + \frac{1}{2^{K_b-1}} \sum_{k=1}^{K/2} \binom{K-1}{K/2-k} \left[\sum_{n=0}^{k-1} \exp\left(-\frac{KE_s}{2N_0}\right) \frac{(KE_s/2N_0)^n}{n!} - 1 \right] \quad (5-21)$$

Noting that

$$\sum_{k=1}^{K/2} \binom{K-1}{K/2-k} = 2^{K-2} \quad (5-22)$$

then Eq. (5-21) further simplifies to

$$P_M(1) = \frac{1}{2^{K-1}} \sum_{k=1}^{K/2} \binom{K-1}{K/2-k} \sum_{n=0}^{k-1} \exp\left(-\frac{KE_s}{2N_0}\right) \frac{(KE_s/2N_0)^n}{n!} \quad (5-23)$$

To compute the probability of choosing NRZ when in fact Manchester is the true encoding, we need to evaluate $\Pr\{D \geq 0\} = 1 - \Pr\{D < 0\}$ when instead of Eq. (5-15) we have

$$\begin{aligned} \bar{X}_k &= (c_k + jc_{k+1}) \sqrt{\frac{P}{8}} T \\ \bar{Y}_k &= -(c_k + jc_{k+1}) \sqrt{\frac{P}{8}} T \end{aligned} \quad (5-24)$$

Since the impact of the negative mean for \bar{Y}_k in Eq. (5-24) is to reverse the sign of ξ_2 in Eq. (5-18), then we immediately conclude that for this case the values of a and b in Eq. (5-19) merely switch roles, i.e.,

$$a = \sqrt{K \left(\frac{E_s}{N_0} \right)} \quad (5-25)$$

$$b = 0$$

Substituting these values in Eq. (5-16) now gives

$$\begin{aligned} P_M(2) &= \\ &1 - \left\{ \frac{1}{2} + \frac{1}{2^{K-1}} \sum_{k=1}^{K/2} \binom{K-1}{K/2-k} \left[1 - \sum_{n=0}^{k-1} \exp\left(-\frac{KE_s}{2N_0}\right) \frac{(KE_s/2N_0)^n}{n!} \right] \right\} \end{aligned} \quad (5-26)$$

which again simplifies to

$$P_M(2) = \frac{1}{2^{K-1}} \sum_{k=1}^{K/2} \binom{K-1}{K/2-k} \sum_{n=0}^{k-1} \exp\left(-\frac{KE_s}{2N_0}\right) \frac{(KE_s/2N_0)^n}{n!} \quad (5-27)$$

Since Eqs. (5-23) and (5-27) are identical, the average probability of mismatch, P_M , is then either of the two results.

Illustrated in Fig. 5-2 are numerical results for the misclassification probability obtained by computer simulation for the optimum and reduced-complexity data format classifiers as given by Eqs. (5-8), (5-11) and (5-12). Also illustrated are the numerical results obtained from the closed-form analytical solution given in Eq. (5-23) for the low-SNR reduced-complexity scheme. As can be seen, the agreement between theoretical and simulated results is exact. Furthermore, the difference in performance between the optimum and reduced-complexity classifiers is quite small over a large range of SNRs.

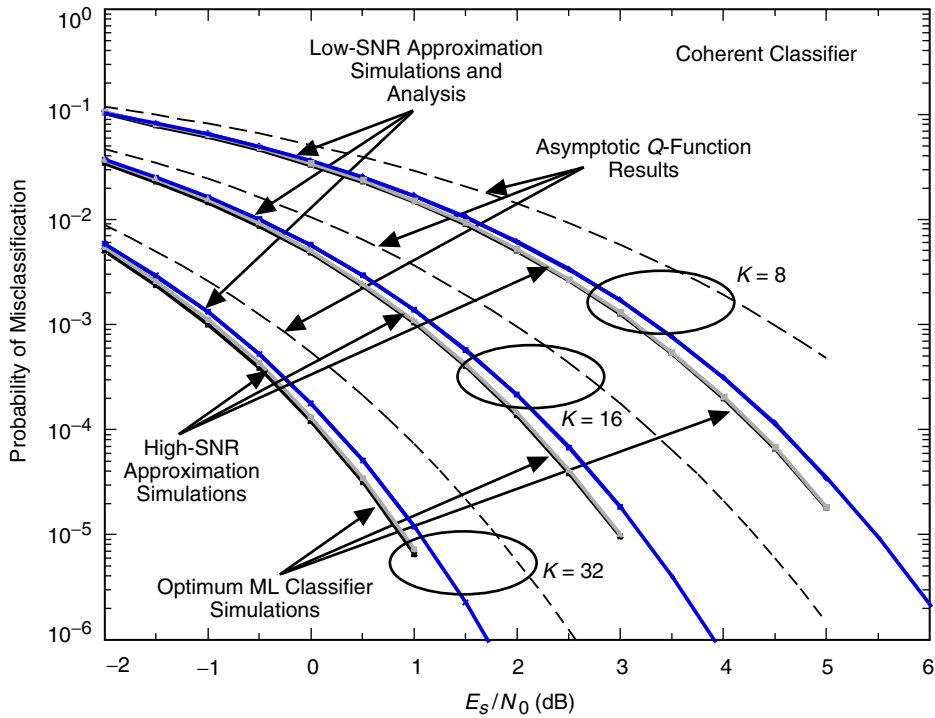


Fig. 5-2. A comparison of the performance of coherent data format classifiers for BPSK modulation.

5.1.3.2 Asymptotic Behavior. To evaluate the asymptotic (large K) behavior of the misclassification probability, we apply the central limit theorem to the quadratic form in Eq. (5-13). Specifically, in the limit of large K , D tends to a Gaussian RV with mean

$$\bar{D} = K \bar{X}_{ck} \bar{Y}_{ck} = \frac{KPT^2}{8} \quad (5-28)$$

and variance

$$\sigma_D^2 = K \text{var} \{X_{ck} Y_{ck}\} = K \left[\overline{X_{ck}^2 Y_{ck}^2} - \bar{X}_{ck}^2 \bar{Y}_{ck}^2 \right] \quad (5-29)$$

After some manipulation, it can be shown that Eq. (5-29) can be expressed as

$$\begin{aligned} \sigma_D^2 &= K \left[\text{var} \{X_{ck}\} \text{var} \{Y_{ck}\} + \text{var} \{X_{ck}\} \overline{Y_{ck}^2} + \text{var} \{Y_{ck}\} \overline{X_{ck}^2} \right] \\ &= K \left[\left(\frac{N_0 T}{8} \right)^2 + 2 \left(\frac{N_0 T}{8} \right) \left(\frac{PT^2}{8} \right) \right] = K \left(\frac{N_0 T}{8} \right)^2 \left(1 + 2 \frac{E_s}{N_0} \right) \end{aligned} \quad (5-30)$$

Thus, in view of the Gaussian assumption, $P_M = \Pr \{D < 0\}$ is obtained in the form of a Gaussian Q -function, namely,

$$P_M = Q \left(\frac{\bar{D}}{\sigma_D} \right) = Q \left(\sqrt{K \frac{(E_s/N_0)^2}{1 + 2E_s/N_0}} \right) \quad (5-31)$$

The asymptotic misclassification probability of Eq. (5-31) is superimposed on the results in Fig. 5-1.

5.2 Coherent Classifiers of Data Format for QPSK

5.2.1 Maximum-Likelihood Coherent Classifier of Data Format for QPSK

For QPSK modulation, the received signal is given by

$$\begin{aligned}
r(t) &= \sqrt{P} \left(\sum_{n=-\infty}^{\infty} c_n p(t - nT) \right) \cos \omega_c t \\
&\quad + \sqrt{P} \left(\sum_{n=-\infty}^{\infty} b_n p(t - nT) \right) \sin \omega_c t + n(t) \quad (5-32)
\end{aligned}$$

where now $\{c_n\}$ and $\{b_n\}$ are the in-phase (I) and quadrature (Q) sequences of binary iid data taking on values ± 1 with equal probability. For simplicity, we have assumed that the I and Q baseband waveforms have the same data format. For an observation of K symbol intervals, each of duration T , the CLF is given by²

$$\begin{aligned}
&p(r(t)|\{c_n\}, \{b_n\}, p(t)) \\
&= \frac{1}{\sqrt{\pi N_0}} \exp \left\{ -\frac{1}{N_0} \int_0^{KT} \left[r(t) - \sqrt{P} \left(\sum_{n=-\infty}^{\infty} c_n p(t - nT) \right) \cos \omega_c t \right. \right. \\
&\quad \left. \left. - \sqrt{P} \left(\sum_{n=-\infty}^{\infty} b_n p(t - nT) \right) \sin \omega_c t \right]^2 dt \right\} \\
&= C \exp \left(\frac{2\sqrt{P}}{N_0} \sum_{k=0}^{K-1} c_k \int_{kT}^{(k+1)T} r(t) p(t - kT) \cos \omega_c t dt \right) \\
&\quad \times \exp \left(\frac{2\sqrt{P}}{N_0} \sum_{k=0}^{K-1} b_k \int_{kT}^{(k+1)T} r(t) p(t - kT) \sin \omega_c t dt \right) \\
&= C \prod_{k=0}^{K-1} \exp \left(\frac{2\sqrt{P}}{N_0} c_k \int_{kT}^{(k+1)T} r(t) p(t - kT) \cos \omega_c t dt \right) \\
&\quad \times \exp \left(\frac{2\sqrt{P}}{N_0} \sum_{k=0}^{K-1} b_k \int_{kT}^{(k+1)T} r(t) p(t - kT) \sin \omega_c t dt \right) \quad (5-33)
\end{aligned}$$

² As in other chapters, we again assume a system with a fixed modulation bandwidth or, equivalently, a fixed symbol rate. Thus, under this assumption, T , which denotes the duration of a modulation symbol, is equal to two bit times for QPSK and is equal to a single bit time for BPSK.

Averaging over the iid data sequences and taking the logarithm gives the LLF

$$\begin{aligned} \Lambda \triangleq \ln p(r(t) | p(t)) &= \sum_{k=0}^{K-1} \left[\ln \cosh \left(\frac{2\sqrt{P}}{N_0} \int_{kT}^{(k+1)T} r(t) p(t-kT) \cos \omega_c t dt \right) \right. \\ &\quad \left. + \ln \cosh \left(\frac{2\sqrt{P}}{N_0} \int_{kT}^{(k+1)T} r(t) p(t-kT) \sin \omega_c t dt \right) \right] \end{aligned} \quad (5-34)$$

Analogous to Eq. (5-7), defining the received I and Q observables

$$\begin{aligned} r_{ck}(l) &\triangleq \int_{kT}^{(k+1)T} r(t) p_l(t-kT) \cos \omega_c t dt \\ r_{sk}(l) &\triangleq \int_{kT}^{(k+1)T} r(t) p_l(t-kT) \sin \omega_c t dt \end{aligned} \quad (5-35)$$

then the classification rule for choosing the data format is as follows: Choose Manchester encoding if

$$\begin{aligned} \sum_{k=0}^{K-1} \left[\ln \cosh \left(\frac{2\sqrt{P}}{N_0} r_{ck}(1) \right) + \ln \cosh \left(\frac{2\sqrt{P}}{N_0} r_{sk}(1) \right) \right] < \\ \sum_{k=0}^{K-1} \left[\ln \cosh \left(\frac{2\sqrt{P}}{N_0} r_{ck}(2) \right) + \ln \cosh \left(\frac{2\sqrt{P}}{N_0} r_{sk}(2) \right) \right] \end{aligned} \quad (5-36)$$

Otherwise, choose NRZ.

5.2.2 Reduced-Complexity Data Format QPSK Classifiers

Here again we may simplify the form of the classification rule in Eq. (5-36) by using the nonlinearity approximations in Eq. (5-9). For example, for low SNR, the classification decision would be based on the inequality

$$\sum_{k=0}^{K-1} \left[\int_{kT}^{(k+1/2)T} r(t) \cos \omega_c t dt \int_{(k+1/2)T}^{(k+1)T} r(\tau) \cos \omega_c \tau d\tau + \int_{kT}^{(k+1/2)T} r(t) \sin \omega_c t dt \int_{(k+1/2)T}^{(k+1)T} r(\tau) \sin \omega_c \tau d\tau \right] < 0 \quad (5-37)$$

Figure 5-3 illustrates the implementation of the classifier defined above.

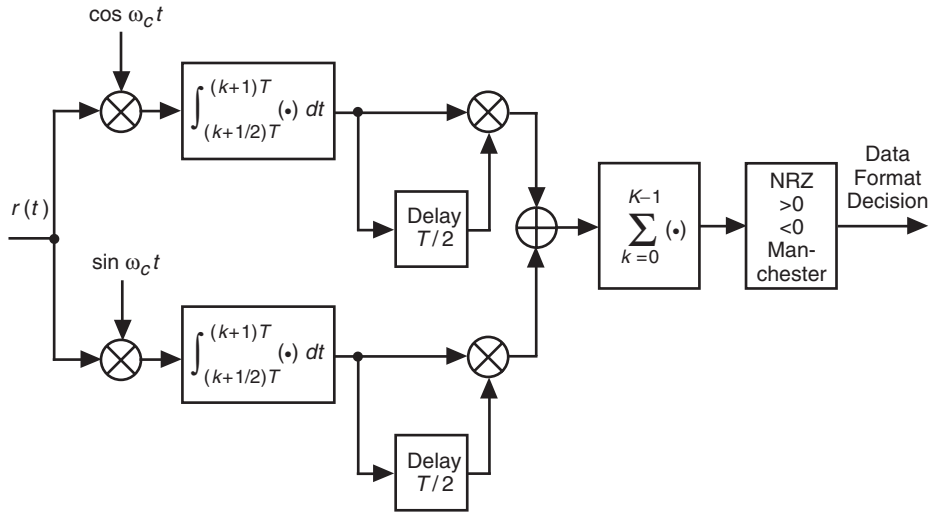


Fig. 5-3. Reduced-complexity coherent data format classifiers for QPSK modulation, for low SNR.

5.2.3 Probability of Misclassification for Coherent QPSK

Defining $X_{sk} = \int_{kT}^{(k+1/2)T} r(t) \sin \omega_c t dt$, $Y_{sk} = \int_{(k+1/2)T}^{(k+1)T} r(\tau) \sin \omega_c \tau d\tau$; $k = 0, 1, \dots, K-1$, and assigning them to the complex Gaussian RVs $X_{k+K/2} = X_{sk} + jX_{s,k+1}$, $Y_{k+K/2} = Y_{sk} + jY_{s,k+1}$, then analogous to Eq. (5-14) we can write

$$D = \frac{1}{2} \sum_{k=0}^{K-1} (X_k Y_k^* + X_k^* Y_k) \quad (5-38)$$

where the means of the observables are now given by

$$\bar{X}_k = \bar{Y}_k = (a_k + ja_{k+1}) \sqrt{P/16T}; \quad k = 0, 1, \dots, K/2 - 1 \quad (5-39)$$

$$\bar{X}_k = \bar{Y}_k = (b_k + jb_{k+1}) \sqrt{P/16T}; \quad k = K/2, K/2 + 1, \dots, K - 1$$

Since all the observables are again mutually iid Gaussian RVs, then the LLF in Eq. (5-38) is still a quadratic form of Gaussian RVs and the probability $\Pr\{D < 0\}$ can be evaluated in closed form in the same manner as before. Note that because of the assumption of a fixed modulation bandwidth the probabilities of misclassification for BPSK and QPSK are different, whereas had we assumed an equivalence between the information (bit) rates of the two modulations, these probabilities would have become equal.

Before moving on to a discussion of noncoherent data format classification schemes, it is of interest to ask whether there exists a universal classification rule that for a given symbol rate (modulation bandwidth) is appropriate (but not necessarily optimum) for M -ary phase-shift keying (M -PSK) independent of the value of M . This would allow determination of the data format prior to modulation classification, which for M -PSK constitutes determining the value of M . Before answering this question, we first point out that the low SNR ML classification rule of Eq. (5-37), which is explicitly derived for QPSK modulation, also would work for BPSK, albeit with a penalty in performance relative to the ML rule of Eq. (5-11) due to the presence now of a noise-only term in the quadrature channel. Having said this, it also can be demonstrated that the classification rule of Eq. (5-37), which can be viewed as the extension of the classification rule in Eq. (5-11) to complex observables, is also suitable for M -PSK ($M > 4$), and furthermore the misclassification performance of this scheme still would be given by Eq. (5-23) independent now of the value of M .

5.3 Noncoherent Classification of Data Format for BPSK

5.3.1 Maximum-Likelihood Noncoherent Classifier of Data Format for BPSK

Here we assume that the carrier has a time-invariant random phase, θ_c , that is unknown and uniformly distributed. Thus, the received signal of Eq. (5-1) is now modeled as

$$r(t) = \sqrt{2P} \left(\sum_{n=-\infty}^{\infty} c_n p(t - nT) \right) \cos(\omega_c t + \theta_c) + n(t) \quad (5-40)$$

and the corresponding CLF becomes

$$p(r(t)|\{c_n\}, p(t), \theta_c) = C \prod_{k=0}^{K-1} \exp \left(\frac{2\sqrt{2P}}{N_0} c_k \int_{kT}^{(k+1)T} r(t) p(t - kT) \cos(\omega_c t + \theta_c) dt \right) \quad (5-41)$$

At this point, we have the option of first averaging over the random carrier phase and then the data or vice versa. Considering the first option, we start by rewriting Eq. (5-41) as

$$p(r(t)|\{c_n\}, p(t), \theta_c) = C \exp \left(\frac{2\sqrt{2P}}{N_0} \sqrt{\left(\sum_{k=0}^{K-1} c_k r_{ck} \right)^2 + \left(\sum_{k=0}^{K-1} c_k r_{sk} \right)^2} \cos(\theta_c + \eta) \right) \quad (5-42)$$

$$\eta = \tan^{-1} \frac{\sum_{k=0}^{K-1} c_k r_{sk}}{\sum_{k=0}^{K-1} c_k r_{ck}}$$

Averaging over the carrier phase results in (ignoring constants)

$$p(r(t)|\{c_n\}, p(t)) = I_0 \left(\frac{2\sqrt{2P}}{N_0} \sqrt{\left(\sum_{k=0}^{K-1} c_k r_{ck} \right)^2 + \left(\sum_{k=0}^{K-1} c_k r_{sk} \right)^2} \right) \quad (5-43)$$

where $I_0(\cdot)$ is the zero-order modified Bessel function of the first kind. Unfortunately, the average over the data sequence cannot be obtained in closed form. Hence, the classification algorithm can be stated only as follows: Given that NRZ was transmitted, choose the Manchester format if

$$E_{\mathbf{c}} \left\{ I_0 \left(\frac{2\sqrt{2P}}{N_0} \sqrt{\left(\sum_{k=0}^{K-1} c_k r_{ck}(1) \right)^2 + \left(\sum_{k=0}^{K-1} c_k r_{sk}(1) \right)^2} \right) \right\} <$$

$$E_{\mathbf{c}} \left\{ I_0 \left(\frac{2\sqrt{2P}}{N_0} \sqrt{\left(\sum_{k=0}^{K-1} c_k r_{ck}(2) \right)^2 + \left(\sum_{k=0}^{K-1} c_k r_{sk}(2) \right)^2} \right) \right\} \quad (5-44)$$

where $E_{\mathbf{c}}\{\cdot\}$ denotes expectation over the data sequence $\mathbf{c} = (c_0, c_1, \dots, c_{K-1})$. Otherwise, choose NRZ.

Consider now the second option, where we first average over the data sequence. Then,

$$\begin{aligned}
& p(r(t)|p(t), \theta_c) \\
&= C \prod_{k=0}^{K-1} E_{c_k} \left\{ \exp \left(\frac{2\sqrt{2P}}{N_0} c_k \int_{kT}^{(k+1)T} r(t) p(t - kT) \cos(\omega_c t + \theta_c) dt \right) \right\} \\
&= C \exp \left[\ln \left(\prod_{k=0}^{K-1} E_{c_k} \left\{ \exp \left(\frac{2\sqrt{2P}}{N_0} c_k \right. \right. \right. \right. \\
&\quad \left. \left. \left. \times \int_{kT}^{(k+1)T} r(t) p(t - kT) \cos(\omega_c t + \theta_c) dt \right) \right\} \right) \right] \\
&= C \exp \left[\sum_{k=0}^{K-1} \ln \left(E_{c_k} \left\{ \exp \left(\frac{2\sqrt{2P}}{N_0} c_k \right. \right. \right. \right. \right. \\
&\quad \left. \left. \left. \times \int_{kT}^{(k+1)T} r(t) p(t - kT) \cos(\omega_c t + \theta_c) dt \right) \right\} \right) \right] \\
&= C \exp \left[\sum_{k=0}^{K-1} \ln \cosh \left(\frac{2\sqrt{2P}}{N_0} \int_{kT}^{(k+1)T} r(t) p(t - kT) \cos(\omega_c t + \theta_c) dt \right) \right]
\end{aligned} \tag{5-45}$$

Thus, a classification between NRZ and Manchester encoding would be based on a comparison of

$$\begin{aligned}
LR &= \\
& \frac{E_{\theta_c} \left\{ \exp \left[\sum_{k=0}^{K-1} \ln \cosh \left(\frac{2\sqrt{2P}}{N_0} \int_{kT}^{(k+1)T} r(t) p_1(t - kT) \cos(\omega_c t + \theta_c) dt \right) \right] \right\}}{E_{\theta_c} \left\{ \exp \left[\sum_{k=0}^{K-1} \ln \cosh \left(\frac{2\sqrt{2P}}{N_0} \int_{kT}^{(k+1)T} r(t) p_2(t - kT) \cos(\omega_c t + \theta_c) dt \right) \right] \right\}}
\end{aligned} \tag{5-46}$$

to unity.

To simplify matters, before averaging over the carrier phase, one must employ the approximations to the nonlinearities given in Eq. (5-9). In particular, for low SNR, we have

$$\begin{aligned}
& p(r(t)|p(t)) \\
&= E_{\theta_c} \left\{ \exp \left[\frac{1}{2} \sum_{k=0}^{K-1} \left(\frac{2\sqrt{2P}}{N_0} \int_{kT}^{(k+1)T} r(t) p(t-kT) \cos(\omega_c t + \theta_c) dt \right)^2 \right] \right\} \\
&= E_{\theta_c} \left\{ \exp \left[\frac{4P}{N_0^2} \sum_{k=0}^{K-1} (r_{ck} \cos \theta_c - r_{sk} \sin \theta_c)^2 \right] \right\} \\
&= E_{\theta_c} \left\{ \exp \left[\frac{4P}{N_0^2} \sum_{k=0}^{K-1} (r_{ck}^2 + r_{sk}^2) \cos^2(\theta_c + \eta_k) \right] \right\} \\
&= \exp \left[\frac{2P}{N_0^2} \sum_{k=0}^{K-1} (r_{ck}^2 + r_{sk}^2) \right] \\
&\quad \times E_{\theta_c} \left\{ \exp \left[\left(\frac{2P}{N_0^2} \sum_{k=0}^{K-1} (r_{ck}^2 + r_{sk}^2) \cos(2(\theta_c + \eta_k)) \right) \right] \right\} \\
&= \exp \left[\frac{2P}{N_0^2} \sum_{k=0}^{K-1} (r_{ck}^2 + r_{sk}^2) \right] \\
&\quad \times E_{\theta_c} \left\{ \exp \left[\left(\frac{2P}{N_0^2} \left(\cos 2\theta_c \sum_{k=0}^{K-1} (r_{ck}^2 + r_{sk}^2) \cos 2\eta_k \right. \right. \right. \\
&\quad \left. \left. \left. - \sin 2\theta_c \sum_{k=0}^{K-1} (r_{ck}^2 + r_{sk}^2) \sin 2\eta_k \right) \right) \right] \right\} \\
&= \exp \left[\frac{2P}{N_0^2} \sum_{k=0}^{K-1} (r_{ck}^2 + r_{sk}^2) \right] \\
&\quad \times I_0 \left(\frac{2P}{N_0^2} \sqrt{\left(\sum_{k=0}^{K-1} (r_{ck}^2 + r_{sk}^2) \cos 2\eta_k \right)^2 + \left(\sum_{k=0}^{K-1} (r_{ck}^2 + r_{sk}^2) \sin 2\eta_k \right)^2} \right)
\end{aligned} \tag{5-47}$$

where

$$\eta_k = \tan^{-1} \frac{r_{sk}}{r_{ck}} \quad (5-48)$$

Thus, since

$$\begin{aligned} \cos 2\eta_k &= \frac{r_{ck}^2 - r_{sk}^2}{r_{ck}^2 + r_{sk}^2} \\ \sin 2\eta_k &= \frac{2r_{ck}r_{sk}}{r_{ck}^2 + r_{sk}^2} \end{aligned} \quad (5-49)$$

we finally have

$$\begin{aligned} p(r(t)|p(t)) &= \exp \left[\frac{2P}{N_0^2} \sum_{k=0}^{K-1} (r_{ck}^2 + r_{sk}^2) \right] \\ &\quad \times I_0 \left(\frac{2P}{N_0^2} \sqrt{\left(\sum_{k=0}^{K-1} (r_{ck}^2 - r_{sk}^2) \right)^2 + 4 \left(\sum_{k=0}^{K-1} r_{ck}r_{sk} \right)^2} \right) \\ &= \exp \left[\frac{2P}{N_0^2} \sum_{k=0}^{K-1} (r_{ck}^2 + r_{sk}^2) \right] I_0 \left(\frac{2P}{N_0^2} \left| \sum_{k=0}^{K-1} \tilde{r}_k^2 \right| \right) \end{aligned} \quad (5-50)$$

where

$$\tilde{r}_k \triangleq r_{ck} + jr_{sk} = \int_{kT}^{(k+1)T} r(t) p(t - kT) e^{j\omega_c t} dt \quad (5-51)$$

Finally then, the classification decision rule analogous to Eq. (5-44) is: Given that NRZ data were transmitted, decide on Manchester coding if

$$\begin{aligned} \exp \left[\frac{2P}{N_0^2} \sum_{k=0}^{K-1} |\tilde{r}_k(1)|^2 \right] I_0 \left(\frac{2P}{N_0^2} \left| \sum_{k=0}^{K-1} \tilde{r}_k^2(1) \right| \right) < \\ \exp \left[\frac{2P}{N_0^2} \sum_{k=0}^{K-1} |\tilde{r}_k(2)|^2 \right] I_0 \left(\frac{2P}{N_0^2} \left| \sum_{k=0}^{K-1} \tilde{r}_k^2(2) \right| \right) \end{aligned} \quad (5-52)$$

Equivalently, normalizing the observables to

$$\tilde{r}'_k \triangleq \frac{1}{T} \int_{kT}^{(k+1)T} \frac{r(t)}{\sqrt{2P}} p(t - kT) e^{j\omega_c t} dt \quad (5-53)$$

then Eq. (5-52) becomes

$$\begin{aligned} & \exp \left[\left(\frac{2E_s}{N_0} \right)^2 \sum_{k=0}^{K-1} |\tilde{r}'_k(1)|^2 \right] I_0 \left(\left(\frac{2E_s}{N_0} \right)^2 \left| \sum_{k=0}^{K-1} \tilde{r}'_k{}^2(1) \right| \right) < \\ & \exp \left[\left(\frac{2E_s}{N_0} \right)^2 \sum_{k=0}^{K-1} |\tilde{r}'_k(2)|^2 \right] I_0 \left(\left(\frac{2E_s}{N_0} \right)^2 \left| \sum_{k=0}^{K-1} \tilde{r}'_k{}^2(2) \right| \right) \end{aligned} \quad (5-54)$$

Since we have already assumed low SNR in arriving at Eq. (5-54), we can further approximate the nonlinearities in that equation by their values for small arguments. Retaining only linear terms, we arrive at the simplification

$$\sum_{k=0}^{K-1} |\tilde{r}'_k(1)|^2 < \sum_{k=0}^{K-1} |\tilde{r}'_k(2)|^2 \quad (5-55)$$

or, equivalently,

$$\sum_{k=0}^{K-1} |\tilde{r}_k(1)|^2 < \sum_{k=0}^{K-1} |\tilde{r}_k(2)|^2 \quad (5-56)$$

which again does not require knowledge of SNR. On the other hand, if we retain second-order terms, then Eq. (5-54) simplifies to

$$\begin{aligned} & \sum_{k=0}^{K-1} |\tilde{r}'_k(1)|^2 + \frac{1}{4} \left(\frac{2E_s}{N_0} \right)^2 \left[2 \left(\sum_{k=0}^{K-1} |\tilde{r}'_k(1)|^2 \right)^2 + \left| \sum_{k=0}^{K-1} \tilde{r}'_k{}^2(1) \right|^2 \right] < \\ & \sum_{k=0}^{K-1} |\tilde{r}'_k(2)|^2 + \frac{1}{4} \left(\frac{2E_s}{N_0} \right)^2 \left[2 \left(\sum_{k=0}^{K-1} |\tilde{r}'_k(2)|^2 \right)^2 + \left| \sum_{k=0}^{K-1} \tilde{r}'_k{}^2(2) \right|^2 \right] \end{aligned} \quad (5-57)$$

which is SNR-dependent.

Expanding Eq. (5-56) in the form of Eq. (5-10), we obtain

$$\begin{aligned} & \sum_{k=0}^{K-1} \left(\int_{kT}^{(k+1)T} r(t) \cos \omega_c t dt \right)^2 + \left(\int_{kT}^{(k+1)T} r(t) \sin \omega_c t dt \right)^2 < \\ & \sum_{k=0}^{K-1} \left(\int_{kT}^{(k+1/2)T} r(t) \cos \omega_c t dt - \int_{(k+1/2)T}^{(k+1)T} r(t) \cos \omega_c t dt \right)^2 \\ & + \sum_{k=0}^{K-1} \left(\int_{kT}^{(k+1/2)T} r(t) \sin \omega_c t dt - \int_{(k+1/2)T}^{(k+1)T} r(t) \sin \omega_c t dt \right)^2 \end{aligned}$$

or

$$\begin{aligned} & \sum_{k=0}^{K-1} \int_{kT}^{(k+1/2)T} r(t) \cos \omega_c t dt \int_{(k+1/2)T}^{(k+1)T} r(\tau) \cos \omega_c \tau d\tau \\ & + \sum_{k=0}^{K-1} \int_{kT}^{(k+1/2)T} r(t) \sin \omega_c t dt \int_{(k+1/2)T}^{(k+1)T} r(\tau) \sin \omega_c \tau d\tau < 0 \\ & = \operatorname{Re} \left\{ \sum_{k=0}^{K-1} \int_{kT}^{(k+1/2)T} r(t) e^{j\omega_c t} dt \int_{(k+1/2)T}^{(k+1)T} r(\tau) e^{-j\omega_c \tau} d\tau \right\} < 0 \quad (5-58) \end{aligned}$$

which is the analogous result to Eq. (5-11) for the coherent case.

For high SNR, even after applying the approximations to the nonlinearities given in Eq. (5-9), it is still difficult to average over the random carrier phase. Instead, we take note of the resemblance between Eqs. (5-58) and (5-59) for the low SNR case and propose an ad hoc complex equivalent to Eq. (5-12) for the noncoherent high SNR case, namely,

$$\begin{aligned} & \sum_{k=0}^{K-1} \left| \int_{kT}^{(k+1/2)T} r(t) e^{j\omega_c t} dt + \int_{(k+1/2)T}^{(k+1)T} r(t) e^{j\omega_c t} dt \right| < \\ & \sum_{k=0}^{K-1} \left| \int_{kT}^{(k+1/2)T} r(t) e^{j\omega_c t} dt - \int_{(k+1/2)T}^{(k+1)T} r(t) e^{j\omega_c t} dt \right| \quad (5-59) \end{aligned}$$

Figure 5-4 is a block diagram of the implementation of the low and high SNR classifiers defined by Eqs. (5-58) and (5-59).

5.3.2 Probability of Misclassification for Noncoherent BPSK

To compute the probability of misclassification, we note that Eq. (5-58) is still made up of a sum of products of mutually independent real Gaussian RVs and thus can still be written in the form of Eq. (5-14) with twice as many terms, i.e.,

$$D = \frac{1}{2} \sum_{k=0}^{K-1} (X_k Y_k^* + X_k^* Y_k) \tag{5-60}$$

where now the complex Gaussian RVs are defined as $X_k = X_{ck} + jX_{sk}$, $Y_k = Y_{ck} + jY_{sk}$. The means of the terms are given by

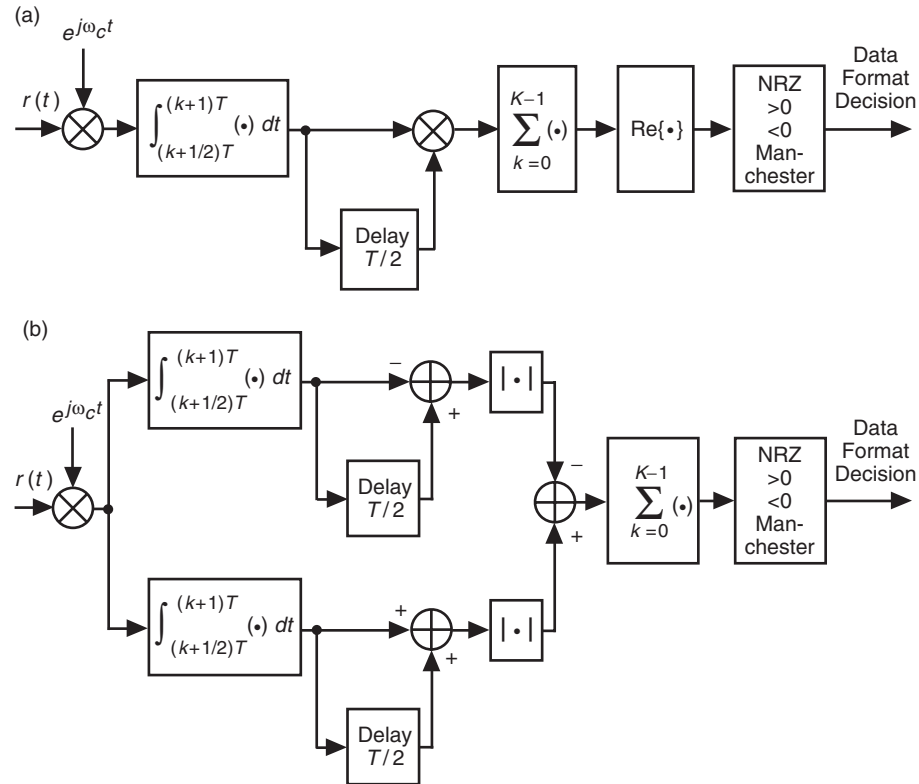


Fig. 5-4. Reduced-complexity noncoherent data format classifiers for BPSK modulation: (a) low SNR and (b) high SNR.

$$\bar{X}_k = \bar{Y}_k = c_k (\cos \theta_c - j \sin \theta_c) \sqrt{P/8T} \quad (5-61)$$

whereas the variances and cross-correlations are the same as in Eq. (5-15). Thus, since the magnitude of the means in Eq. (5-61) is reduced by a factor of $\sqrt{2}$ relative to that of the means in Eq. (5-15), we conclude that the probability of misclassification is obtained from Eq. (5-23) by replacing E_s/N_0 with $E_s/(2N_0)$ and K with $2K$, resulting in

$$P_M = \frac{1}{2^{2K-1}} \sum_{k=1}^K \binom{2K-1}{K-k} \sum_{n=0}^{k-1} \exp\left(-\frac{KE_s}{2N_0}\right) \frac{(KE_s/2N_0)^n}{n!} \quad (5-62)$$

Furthermore, the asymptotic behavior of Eq. (5-62) for large K can be determined from Eq. (5-31) by making the same replacements as above, resulting in

$$P_M = Q\left(\sqrt{\frac{K(E_s/N_0)^2}{2 + 2E_s/N_0}}\right) \quad (5-63)$$

which for sufficiently large E_s/N_0 approaches Eq. (5-31) for the coherent case.

Figure 5-5 illustrates numerical results for the misclassification probability obtained by computer simulation for the low SNR and high SNR reduced-complexity data format classifiers as specified by Eqs. (5-58) and (5-59), respectively, as well as the optimum classifier described by Eq. (5-46). Also illustrated are the numerical results obtained from the closed-form analytical solution given in Eq. (5-62) for the low SNR reduced-complexity scheme (which are in exact agreement with the simulation results) and the asymptotic results obtained from Eq. (5-63). As in the coherent case, the difference in performance between the low and high SNR reduced-complexity classifiers is again quite small over a large range of SNRs. Furthermore, we see here again that the performances of the approximate but simpler classification algorithms are in close proximity to that of the optimum one. Finally, comparison between the corresponding coherent and noncoherent classifiers is illustrated in Fig. 5-6 and reveals a penalty of approximately 1 dB or less depending on the SNR.

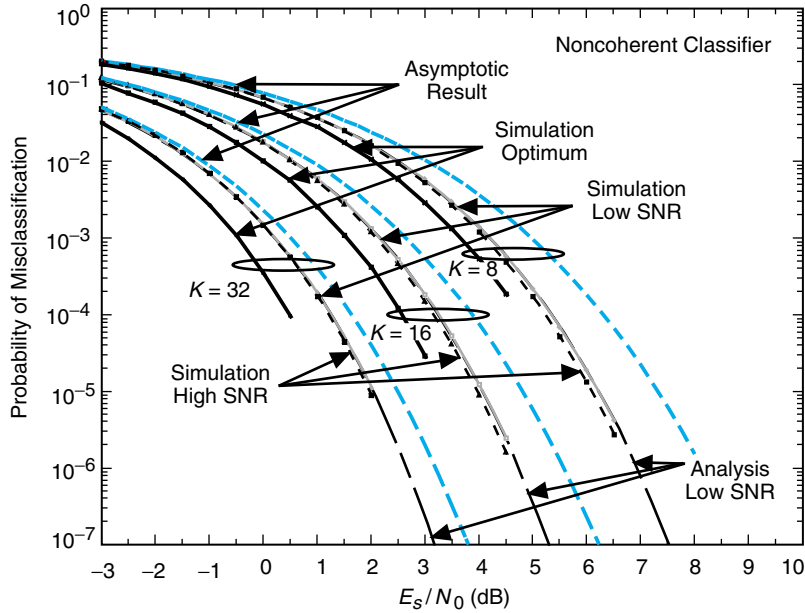


Fig. 5-5. A comparison of the performance of noncoherent data format classifiers for BPSK modulation.

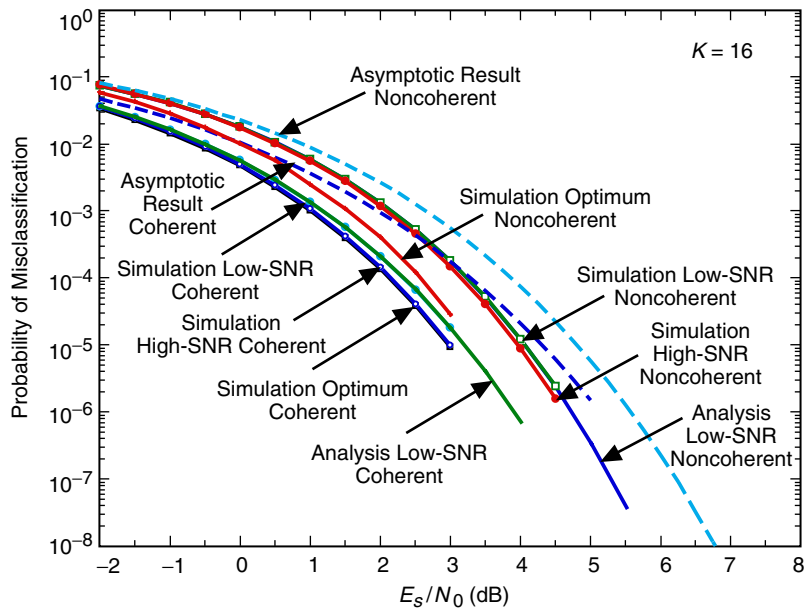


Fig. 5-6. A comparison of the performance of coherent and noncoherent data format classifiers for BPSK modulation: suppressed-carrier case.

5.4 Maximum-Likelihood Noncoherent Classifier of Data Format for QPSK

Following the same approach as in Section 5.2.1, the LLF for the noncoherent QPSK case is easily shown to be

$$\Lambda \triangleq \ln p(r(t)|p(t)) \quad (5-64)$$

$$= \frac{E}{\theta_c} \left\{ \exp \left(\sum_{k=0}^{K-1} \left[\ln \cosh \left(\frac{2\sqrt{P}}{N_0} \int_{kT}^{(k+1)T} r(t) p(t-kT) \cos(\omega_c t + \theta_c) dt \right) + \ln \cosh \left(\frac{2\sqrt{P}}{N_0} \int_{kT}^{(k+1)T} r(t) p(t-kT) \sin(\omega_c t + \theta_c) dt \right) \right] \right) \right\} \quad (5-65)$$

Making the same small argument approximations to the nonlinearities, we get

$$\begin{aligned} p(r(t)|p(t)) &= \frac{E}{\theta_c} \left\{ \exp \left[\frac{1}{2} \sum_{k=0}^{K-1} \left(\frac{2\sqrt{P}}{N_0} \int_{kT}^{(k+1)T} r(t) p(t-kT) \cos(\omega_c t + \theta_c) dt \right)^2 \right. \right. \\ &\quad \left. \left. + \frac{1}{2} \sum_{k=0}^{K-1} \left(\frac{2\sqrt{P}}{N_0} \int_{kT}^{(k+1)T} r(t) p(t-kT) \sin(\omega_c t + \theta_c) dt \right)^2 \right] \right\} \\ &= \frac{E}{\theta_c} \left\{ \exp \left[\frac{2P}{N_0^2} \sum_{k=0}^{K-1} (r_{ck} \cos \theta_c - r_{sk} \sin \theta_c)^2 \right. \right. \\ &\quad \left. \left. + \frac{2P}{N_0^2} \sum_{k=0}^{K-1} (r_{ck} \sin \theta_c + r_{sk} \cos \theta_c)^2 \right] \right\} \\ &= \frac{E}{\theta_c} \left\{ \exp \left[\frac{2P}{N_0^2} \sum_{k=0}^{K-1} (r_{ck}^2 + r_{sk}^2) \cos^2(\theta_c + \eta_k) \right. \right. \\ &\quad \left. \left. + \frac{2P}{N_0^2} \sum_{k=0}^{K-1} (r_{ck}^2 + r_{sk}^2) \sin^2(\theta_c + \eta_k) \right] \right\} \\ &= \exp \left[\frac{2P}{N_0^2} \sum_{k=0}^{K-1} (r_{ck}^2 + r_{sk}^2) \right] \quad (5-66) \end{aligned}$$

Comparing Eq. (5-66) with Eq. (5-50), we note the absence of the Bessel function factor. However, in arriving at Eq. (5-56), which was based on retaining only linear terms, we approximated this factor by unity. Thus, applying the same small argument approximation of the exponential as before, we again arrive at a classification based on Eq. (5-56). Finally then, as in the coherent case, we conclude that the performance of the noncoherent classifier of data format for QPSK is identical to that for BPSK.

5.5 Maximum-Likelihood Coherent Classifier of Data Format for BPSK with Residual and Suppressed Carriers

When NRZ is transmitted, the received signal takes the form of Eq. (5-1) with $p(t) = p_1(t)$ and $P = P_t$, where P_t now denotes the total transmitted power. On the other hand, when Manchester-coded data are transmitted, the received signal has the form

$$r(t) = \sqrt{2P_c} \sin \omega_c t + \sqrt{2P_d} \left(\sum_{n=-\infty}^{\infty} c_n p_2(t - nT) \right) \cos \omega_c t + n(t) \quad (5-67)$$

where $P_c = P_t \cos^2 \beta$ and $P_d = P_t \sin^2 \beta$ are, respectively, the powers allocated to the discrete and data-modulated carriers with β the phase modulation index. Then, analogous to Eq. (5-2), it is straightforward to show that

$$\begin{aligned} p(r(t) | \{c_n\}, p_2(t)) &= C \prod_{k=0}^{K-1} \exp \left(\frac{2\sqrt{2P_c}}{N_0} \int_{kT}^{(k+1)T} r(t) \sin \omega_c t dt \right) \\ &\quad \times \exp \left(\frac{2\sqrt{2P_d}}{N_0} c_k \int_{kT}^{(k+1)T} r(t) p_2(t - kT) \cos \omega_c t dt \right) \end{aligned} \quad (5-68)$$

Averaging over the iid data sequence and taking the logarithm gives

$$\begin{aligned} \ln p(r(t) | p(t)) &= \sum_{k=0}^{K-1} \frac{2\sqrt{2P_c}}{N_0} \int_{kT}^{(k+1)T} r(t) \sin \omega_c t dt \\ &\quad + \sum_{k=0}^{K-1} \ln \cosh \left(\frac{2\sqrt{2P_d}}{N_0} \int_{kT}^{(k+1)T} r(t) p_2(t - kT) \cos \omega_c t dt \right) \end{aligned} \quad (5-69)$$

Finally then, we obtain the classification rule:

Choose Manchester coding if

$$\begin{aligned} \sum_{k=0}^{K-1} \ln \cosh \left(\frac{2\sqrt{2P_t}}{N_0} \int_{kT}^{(k+1)T} r(t) p_1(t - kT) \cos \omega_c t dt \right) < \\ \sum_{k=0}^{K-1} \frac{2\sqrt{2P_c}}{N_0} \int_{kT}^{(k+1)T} r(t) \sin \omega_c t dt \\ + \sum_{k=0}^{K-1} \ln \cosh \left(\frac{2\sqrt{2P_d}}{N_0} \int_{kT}^{(k+1)T} r(t) p_2(t - kT) \cos \omega_c t dt \right) \end{aligned} \quad (5-70)$$

Otherwise, choose NRZ.

To obtain the reduced-complexity version of Eq. (5-70), we once again use the nonlinearity approximations in Eq. (5-9). For the low SNR case, we get after some manipulation

$$\begin{aligned} D \triangleq \sum_{k=0}^{K-1} \left[\frac{2(P_t - P_d)}{N_0^2} (X_{ck}^2 + Y_{ck}^2) + \frac{4(P_t + P_d)}{N_0^2} X_{ck} Y_{ck} - \frac{\sqrt{2P_c}}{N_0} (X_{sk} + Y_{sk}) \right] \\ < 0 \end{aligned} \quad (5-71)$$

where for convenience of notation as before we have defined

$$\begin{aligned} X_{ck} &= \int_{kT_b}^{(k+1/2)T} r(t) \cos \omega_c t dt, \quad Y_{ck} = \int_{(k+1/2)T}^{(k+1)T} r(\tau) \cos \omega_c t d\tau \\ X_{sk} &= \int_{kT}^{(k+1/2)T} r(t) \sin \omega_c t dt, \quad Y_{sk} = \int_{(k+1/2)T}^{(k+1)T} r(\tau) \sin \omega_c t d\tau \end{aligned} \quad (5-72)$$

$k = 0, 1, \dots, K - 1$. Alternatively, in terms of the modulation index, SNR, and normalized observables

$$\begin{aligned}
X'_{ck} &\triangleq \frac{X_{ck}}{T\sqrt{2P_t}}, Y'_{ck} \triangleq \frac{Y_{ck}}{T\sqrt{2P_t}} \\
X'_{sk} &\triangleq \frac{X_{sk}}{T\sqrt{2P_t}}, Y'_{sk} \triangleq \frac{Y_{sk}}{T\sqrt{2P_t}}
\end{aligned} \tag{5-73}$$

Eq. (5-71) becomes

$$\begin{aligned}
D &\triangleq \sum_{k=0}^{K-1} \left[2 \frac{E_t}{N_0} \cos^2 \beta (X'_{ck}{}^2 + Y'_{ck}{}^2) + 4 \frac{E_t}{N_0} (1 + \sin^2 \beta) X'_{ck} Y'_{ck} \right. \\
&\quad \left. - (\cos \beta) (X'_{sk} + Y'_{sk}) \right] < 0
\end{aligned} \tag{5-74}$$

where $E_t/N_0 \triangleq P_t T/N_0$. Although the first two terms in the summation satisfy the type of quadratic form considered in [1, Appendix B], unfortunately, the last term, which does not contain second-order Gaussian RVs, prevents analytically evaluating the misclassification probability in the same manner that was done previously in Section 5.1.3. Nevertheless it is still possible to analytically evaluate the asymptotic (large K) performance in the same manner as before. Here, however, because of the lack of symmetry of the two hypotheses, one must individually evaluate the two misclassification probabilities (probability of choosing Manchester when NRZ is transmitted and vice versa) and then average the resulting expressions.

Considering first the case where NRZ data are transmitted, i.e., the received signal takes the form of Eq. (5-1), then after considerable manipulation, it can be shown that

$$\begin{aligned}
\bar{D} &= \frac{K}{4} \left(\cos^2 \beta + \frac{2E_t}{N_0} \right) \\
\sigma_D^2 &= \frac{K}{8} \frac{N_0}{E_t} \left[\cos^2 \beta + \frac{E_t}{N_0} (1 + \sin^4 \beta) + 4 \left(\frac{E_t}{N_0} \right)^2 \right]
\end{aligned} \tag{5-75}$$

Thus, making the same Gaussian assumption on D , the probability of misclassification for this case is given by

$$\begin{aligned}
P_{M1} &= \Pr\{D < 0\} = Q \left(\frac{\bar{D}}{\sigma_D} \right) \\
&= Q \left(\sqrt{\frac{K \frac{E_t}{N_0} \left(\cos^2 \beta + \frac{2E_t}{N_0} \right)^2}{2 \left[\cos^2 \beta + \frac{E_t}{N_0} (1 + \sin^4 \beta) + 4 \left(\frac{E_t}{N_0} \right)^2 \right]}} \right)
\end{aligned} \tag{5-76}$$

For the case where Manchester-coded data are transmitted, i.e., the received signal takes the form of Eq. (5-67), then again, after considerable manipulation, it can be shown that

$$\begin{aligned}\bar{D} &= -\frac{K}{4} \left(\cos^2 \beta + \frac{2E_t}{N_0} \sin^4 \beta \right) \\ \sigma_D^2 &= \frac{K N_0}{8 E_t} \left[\cos^2 \beta + 2 \frac{E_t}{N_0} \sin^2 \beta + 4 \left(\frac{E_t}{N_0} \right)^2 \sin^6 \beta \right]\end{aligned}\quad (5-77)$$

whereupon the probability of misclassification becomes

$$\begin{aligned}P_{M2} &= \Pr \{D > 0\} = Q \left(-\frac{\bar{D}}{\sigma_D} \right) \\ &= Q \left(\sqrt{\frac{\frac{K E_t}{N_0} \left(\cos^2 \beta + \frac{2E_t}{N_0} \sin^4 \beta \right)^2}{2 \left[\cos^2 \beta + 2 \frac{E_t}{N_0} \sin^2 \beta + 4 \left(\frac{E_t}{N_0} \right)^2 \sin^6 \beta \right]}} \right)\end{aligned}\quad (5-78)$$

Finally, assuming the equiprobable data format hypothesis, the asymptotic average probability of misclassification is the average of Eq. (5-76) and Eq. (5-78), namely,

$$P_M = \frac{1}{2} (P_{M1} + P_{M2}) \quad (5-79)$$

Note that, for $\beta = 90$ deg, $E_t = E_s$ and Eq. (5-79) reduces to Eq. (5-31) as it should.

For high SNR, using the approximation

$$\ln \cosh x \cong |x| - \ln 2 \quad (5-80)$$

we obtain, analogous to Eq. (5-71),

$$D \triangleq \sum_{k=0}^{K-1} \left[\sqrt{P_t} |X_{ck} + Y_{ck}| - \sqrt{P_c} (X_{sk} + Y_{sk}) - \sqrt{P_d} |X_{ck} - Y_{ck}| \right] < 0 \quad (5-81)$$

or in terms of the modulation index and the normalized observables,

$$D \triangleq \sum_{k=0}^{K-1} [|X'_{ck} + Y'_{ck}| - (X'_{sk} + Y'_{sk}) \cos \beta - |X'_{ck} - Y'_{ck}| \sin \beta] < 0 \quad (5-82)$$

Figure 5-7 is an illustration of the average (over the two hypotheses) misclassification probability for the various coherent classification algorithms, where the results are all obtained by computer simulation. We observe that, over a very wide range of SNRs, the performance of the high SNR approximation classifier is virtually a perfect match to that of the optimum classifier, but its implementation is somewhat simpler. On the other hand, while the performance of the low SNR classifier converges to that of the optimum classifier at low SNR as it should, at high SNR it results in considerable degradation. The reasoning behind this relative difference in behavior between the approximate and optimum classifiers can be explained as follows: Whereas at low SNR the maximum difference between $\ln \cosh x$ and its high SNR approximation $|x| - \ln 2$ occurs at $x = 0$ and is equal to $\ln 2$, at high SNR the difference between $\ln \cosh x$ and its low SNR approximation $x^2/2$ grows without bound, i.e., the difference between a linear and a square law behavior. Thus, using the high SNR approximation of $\ln \cosh x$ over the entire range of SNR is a much better fit than using the low SNR approximation over the same SNR range. Illustrated in Fig. 5-8 is a comparison of the performances of the coherent classifiers for the residual- and suppressed-carrier cases, the latter being obtained from the discussion in Section 5.1.1. We observe that for the optimum and high SNR approximation classifiers the two are quite similar in performance although the suppressed-carrier one is a bit inferior. This implies that a discrete carrier component is slightly influential in improving data format classification for coherent communications.

5.6 Maximum-Likelihood Noncoherent Classifier of Data Format for BPSK with Residual and Suppressed Carriers

As in Section 5.3.1, we again assume that the carrier has a random phase, θ_c , that is unknown and uniformly distributed. Then when NRZ is transmitted, the received signal takes the form of Eq. (5-40) with $p(t) = p_1(t)$ and $P = P_t$. On the other hand, when Manchester-coded data are transmitted, the received signal has the form

$$r(t) = \sqrt{2P_c} \sin(\omega_c t + \theta_c) + \sqrt{2P_d} \left(\sum_{n=-\infty}^{\infty} c_n p_2(t - nT) \right) \cos(\omega_c t + \theta_c) + n(t) \quad (5-83)$$

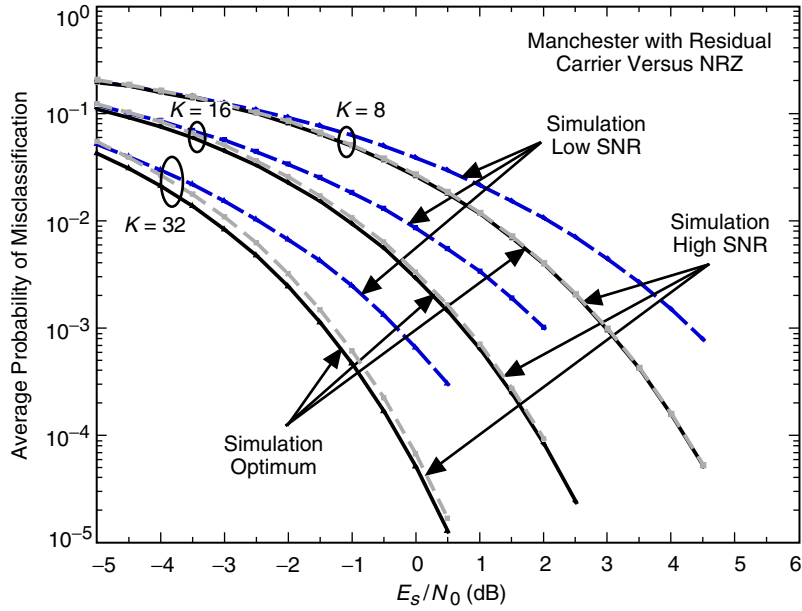


Fig. 5-7. Misclassification probability for residual carrier coherent classifier: $\beta = 60$ deg.

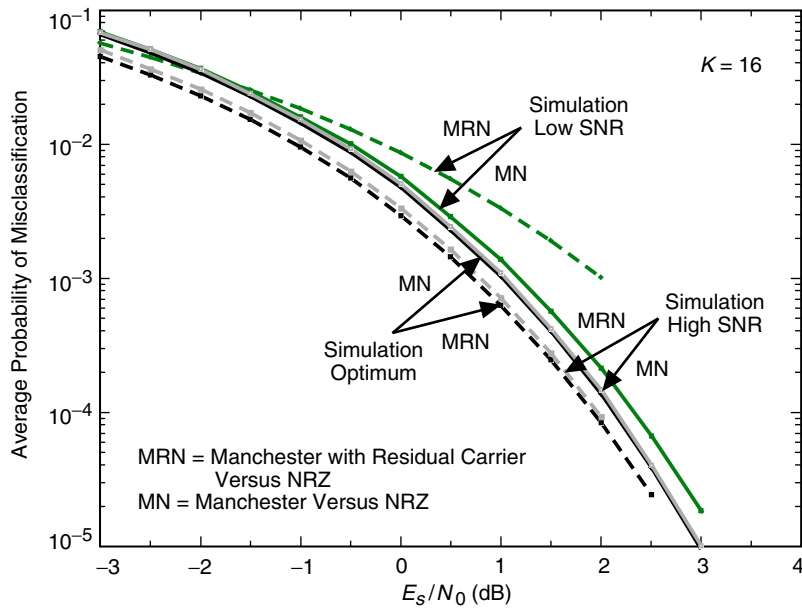


Fig. 5-8. Comparison of misclassification probability for suppressed and residual carrier coherent classifiers.

Without going to great length, following the same procedure as in Section 5.3.1, it is straightforward to show that, analogous to Eq. (5-46), the likelihood ratio for choosing between NRZ and residual-carrier Manchester-coded data is given by

$$\begin{aligned}
LR = & \frac{E_{\theta_c} \left\{ \exp \left[\sum_{k=0}^{K-1} \ln \cosh \left(\frac{2\sqrt{2P_t}}{N_0} \int_{kT}^{(k+1)T} r(t) p_1(t-kT) \cos(\omega_c t + \theta_c) dt \right) \right] \right\}}{E_{\theta_c} \left\{ \exp \left[\sum_{k=0}^{K-1} \ln \cosh \left(\frac{2\sqrt{2P_d}}{N_0} \int_{kT}^{(k+1)T} r(t) p_2(t-kT) \cos(\omega_c t + \theta_c) dt \right) \right] \right\}} \\
& + \frac{2\sqrt{2P_c}}{N_0} \sum_{k=0}^{K-1} \int_{kT}^{(k+1)T} r(t) \sin(\omega_c t + \theta_c) dt \left. \right\} \quad (5-84)
\end{aligned}$$

To obtain a low SNR classifier, we approximate the nonlinearities in Eq. (5-84) by their small argument values which results after considerable simplification in a test analogous to Eq. (5-55) given by the following: Choose Manchester if

$$\sum_{k=0}^{K-1} |\tilde{r}'_k(1)|^2 < (\sin^2 \beta) \sum_{k=0}^{K-1} |\tilde{r}'_k(2)|^2 + (\cos^2 \beta) \left| \sum_{k=0}^{K-1} \tilde{r}'_k(1) \right|^2 \quad (5-85)$$

where as before the real and imaginary components of $\tilde{r}_k(l) = (T_b \sqrt{2P_t}) \tilde{r}'_k(l)$; $l = 1, 2$ are defined in Eq. (5-35). Alternatively, in terms of integrals, Eq. (5-85) becomes

$$\begin{aligned}
& \sum_{k=0}^{K-1} \left| \int_{kT}^{(k+1/2)T} r(t) e^{j\omega_c t} dt + \int_{(k+1/2)T}^{(k+1)T} r(t) e^{j\omega_c t} dt \right|^2 < \\
& (\sin^2 \beta) \sum_{k=0}^{K-1} \left| \int_{kT}^{(k+1/2)T} r(t) e^{j\omega_c t} dt - \int_{(k+1/2)T}^{(k+1)T} r(t) e^{j\omega_c t} dt \right|^2 \\
& + (\cos^2 \beta) \left| \sum_{k=0}^{K-1} \int_{kT}^{(k+1/2)T} r(t) e^{j\omega_c t} dt + \int_{(k+1/2)T}^{(k+1)T} r(t) e^{j\omega_c t} dt \right|^2 \quad (5-86)
\end{aligned}$$

For the high SNR case, by analogy with Eq. (5-86), we propose the ad hoc test

$$\sum_{k=0}^{K-1} \left| \int_{kT}^{(k+1/2)T} r(t) e^{j\omega_c t} dt + \int_{(k+1/2)T}^{(k+1)T} r(t) e^{j\omega_c t} dt \right| <$$

$$(\sin \beta) \sum_{k=0}^{K-1} \left| \int_{kT}^{(k+1/2)T} r(t) e^{j\omega_c t} dt - \int_{(k+1/2)T}^{(k+1)T} r(t) e^{j\omega_c t} dt \right|$$

$$+ (\cos \beta) \left| \sum_{k=0}^{K-1} \int_{kT}^{(k+1/2)T} r(t) e^{j\omega_c t} dt + \int_{(k+1/2)T}^{(k+1)T} r(t) e^{j\omega_c t} dt \right| \quad (5-87)$$

which is consistent with the ad hoc test in Eq. (5-59) when $\beta = 90$ deg.

Analogous to Fig. 5-7, Fig. 5-9 is an illustration of the average misclassification probability for the various classification noncoherent algorithms, where the results are all obtained by computer simulation. We again observe that, over a very wide range of SNRs, the performance of the high SNR approximation

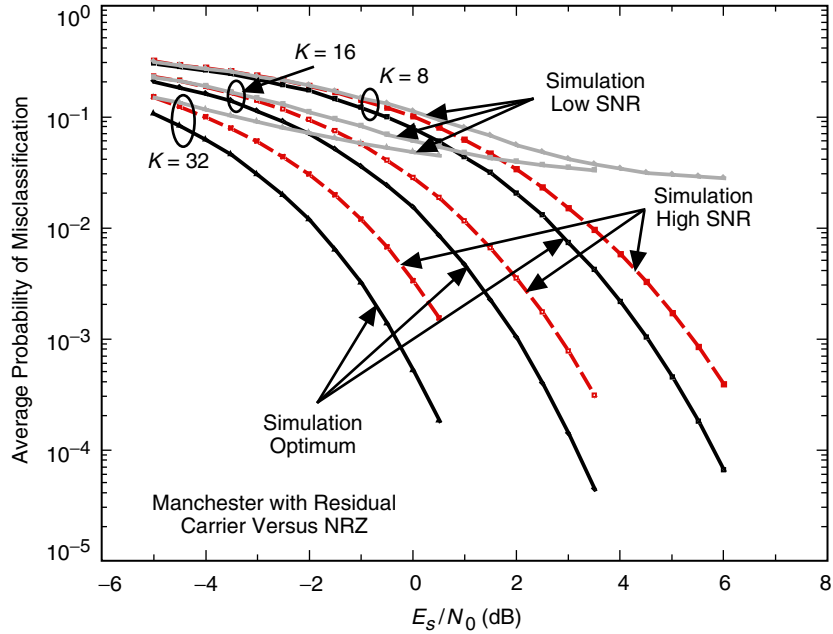


Fig. 5-9. Misclassification probability for residual carrier noncoherent classifier: $\beta = 60$ deg.

classifier is virtually a perfect match to that of the optimum classifier, but its implementation is somewhat simpler. On the other hand, while the performance of the low SNR classifier converges to that of the optimum classifier at low SNR as it should, at high SNR it results in considerable degradation. Illustrated in Fig. 5-10 is a comparison of the performances of the coherent classifiers for the residual- and suppressed-carrier noncoherent classifier cases, the latter being obtained from the discussion in Section 5.3.1 of the chapter. We observe that, as in the coherent comparison illustrated in Fig. 5-8, for the optimum and high SNR approximation classifiers the two are again quite similar in performance, although now the suppressed-carrier one is a bit superior. Finally, analogous to Fig. 5-6, a comparison of the corresponding coherent and noncoherent classifiers for the residual-carrier case is illustrated in Fig. 5-11, and for the optimum metric reveals a penalty of approximately 1.25 dB or less depending on the SNR.

5.7 Maximum-Likelihood Pulse Shape Classification

The solution to the problem of making an ML decision on the pulse shape of a modulation from a variety of different possibilities in principle follows the identical procedure discussed in the previous sections for data format classification, except for the fact that we no longer restrict ourselves to a digital pulse waveform. For example, suppose that we are transmitting a binary modulation, where the pulse shape is known to be one of L possibilities, namely, $p_l(t)$, $l = 1, 2, \dots, L$. Then, using the LLF of Eq. (5-4) and defining $r_k(l)$ as in Eq. (5-7) (without the special cases of NRZ and Manchester), then the ML coherent classifier of pulse shape would be to choose $p_{l^*}(t)$ corresponding to

$$l^* = \underset{l}{\operatorname{argmax}} \sum_{k=0}^{K-1} \ln \cosh \left(\frac{2\sqrt{2P}}{N_0} \int_{kT}^{(k+1)T} r(t) p_l(t - kT) \cos \omega_c t dt \right) \quad (5-88)$$

where the notation $\underset{l}{\operatorname{argmax}} f(l)$ denotes the value of l that maximizes the function $f(l)$. Once again by making small and large argument approximations of the $\ln \cosh(\cdot)$ nonlinearity, one can obtain reduced-complexity classifiers in the same manner as was used in Section 5.1.2 for the special case of data format classification. Other examples involving higher-order modulations follow along the same lines as those just discussed.

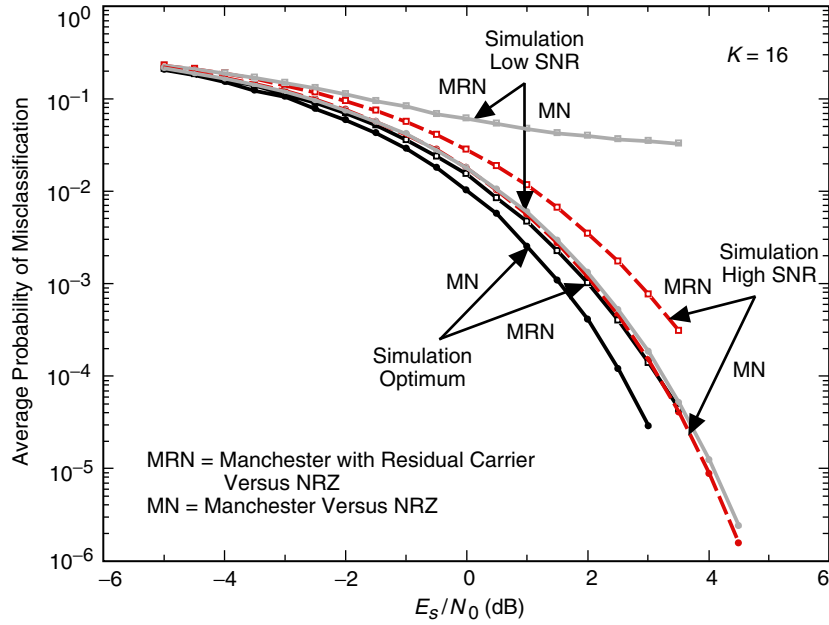


Fig. 5-10. Comparison of misclassification probability for suppressed and residual carrier noncoherent classifiers.

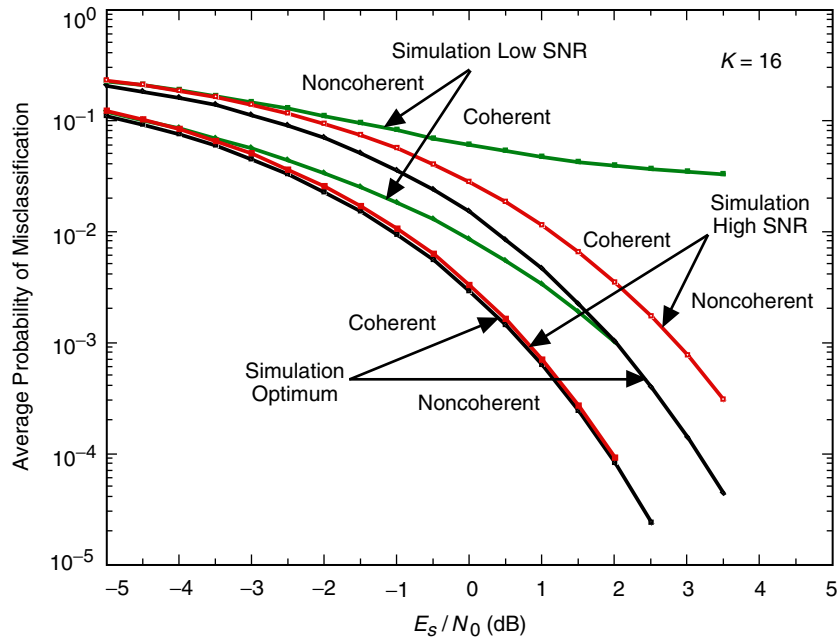


Fig. 5-11. A comparison of performance of coherent and noncoherent data format classifiers for BPSK modulation: residual carrier case.

References

- [1] J. G. Proakis, *Digital Communications*, fourth ed., New York: McGraw Hill, Inc., 2001.
- [2] M. K. Simon and M.-S. Alouini, *Digital Communication over Fading Channels*, second ed., New York: John Wiley & Sons, 2005.